Available online at www.sciencedirect.com
ScienceDirect
Journal of Catalysis 248 (2007) 38–45
JOURNAL OF CATALYSIS
www.elsevier.com/locate/jcat

A density functional theory study of HCN hydrogenation to methylamine on Co(111)

Carolina Oliva [a,*], Co van den Berg [b], J.W. (Hans) Niemantsverdriet [c], Daniel Curulla-Ferré [c,*]

[a] *Research and Technology Chemicals, AkzoNobel Chemicals, Velperweg 76, 6824 BM Arnhem, The Netherlands*
[b] *Research and Technology Chemicals, AkzoNobel Surfactants, Zutphenseweg 10, 7418 AJ Deventer, The Netherlands*
[c] *Technical University of Eindhoven, Den Dolech 2, 5600 MB Eindhoven, The Netherlands*

Received 30 November 2006; revised 21 February 2007; accepted 22 February 2007

Abstract

The hydrogenation of HCN to methylamine on Co(111) was used as a model reaction to study the hydrogenation of nitriles to primary amines. Density functional theory was used to characterize the reaction mechanism, and the results obtained were compared with those for the same reaction on Ni(111). Hydrogen cyanide adsorbs more strongly on Co(111) than on Ni(111), with an adsorption energy of −1.72 eV. The hydrogenation product, methylamine, is weakly adsorbed on Co(111), with an adsorption energy of −0.53 eV, which is very similar to the adsorption energy calculated on Ni(111). The calculated adsorption energies were used to explain the differences in activity and selectivity observed between nickel- and cobalt-based catalysts; the stronger adsorption of HCN on cobalt explains both the lower activity and the higher selectivity observed on this metal. Regarding the reaction mechanism, the hydrogenation reaction implies an imine intermediate (H_2CNH) independent of whether hydrogen reacts with the carbon atom or with the nitrogen atom of the hydrogen cyanide molecule in the first step. The imine intermediate subsequently reacts to form H_3CNH, which is finally hydrogenated to yield methylamine. The overall surface reaction is endothermic. Remarkably, comparing the HCN hydrogenation reaction mechanism on Co(111) and Ni(111) revealed no significant differences.

Keywords: Hydrogenation; Nitriles; Cobalt; Nickel; DFT; Hydrogen cyanide; Methylamine

1. Introduction

The hydrogenation of different nitriles in the liquid phase and at elevated hydrogen pressures is used in the chemicals industry to prepare different important amines. When primary amines are the desired product, the use of nickel and cobalt catalysts is recommended [1]. Although the activity and selectivity of these catalysts are known to differ, the reason for these differences is not yet properly understood [2]. Regarding the reaction mechanism of this process, it is well known that the hydrogenation of nitriles to give primary amines evolves through an imine intermediate, which can condensate with the final primary amine to give secondary amines as byproducts [3]. The formation of secondary amines also involves a secondary imine as an intermediate.

The literature reports a higher content of secondary amines n the literature when a Ni-based catalyst is used instead of a Co-based one; this is valid for both pure metal catalysts and Raney catalysts [1]. In the hydrogenation of palmitonitrile, adiponitrile, and butyronitrile, it was concluded that the higher content in secondary amines observed when using a nickel catalyst instead of a cobalt catalyst was due to the stronger adsorption of the products on nickel. On the other hand, experiments conducted on different nickel and cobalt catalysts for the hydrogenation of lauronitrile showed that the secondary amine was formed by hydrogenation of the secondary imine during the whole experiment on nickel, but at just the end of the reaction on cobalt. The accumulation of the imine intermediate on cobalt in those experiments was explained by a stronger adsorption of the nitrile on this metal [1]. The different adsorption strengths of the nitrile and primary amine were also used to

* Corresponding authors.
E-mail addresses: carolina.oliva.garcia@gmail.com (C. Oliva), d.curulla.ferre@tue.nl (D. Curulla-Ferré).

0021-9517/$ – see front matter
doi:10.1016/j.jcat.2007.02.021

justify the higher selectivity of cobalt catalysts in a study of acetonitrile hydrogenation with nickel and cobalt catalysts alloyed with boron [4]. Other factors have also been considered to justify the differences in selectivity between nickel and cobalt catalyst [1], those studies concluded that selectivity does not depend on the method of catalyst preparation, support used, or catalyst concentration; although there is still some discussion about the effect of the support [2,5].

Although the selectivity toward primary amine formation is higher on Co than on Ni, activity is lower on the former. The initial reaction rate (as the rate of hydrogen consumption) per unit surface area of the metal is 20:10:1 for Ni, Co, and Cu [1]. This observation has also been explained in terms of stronger adsorption of the nitrile reactant on cobalt, which may inhibit the competitive hydrogen adsorption, giving a lower activity on this metal [4].

To summarize, the differences in activity and selectivity observed experimentally in the hydrogenation of nitriles to primary amines between nickel and cobalt-based catalysts have been explained by the following arguments: (1) the stronger adsorption of the nitrile on cobalt accounts for the lower activity on cobalt-based catalysts; (2) the stronger adsorption of the nitrile on cobalt also accounts for the larger selectivity toward primary amines of cobalt catalysts by impeding condensation reactions between the intermediate imine and primary amines to secondary amines; and (3) the selectivity toward primary amines is greater on cobalt catalysts because the primary amine is less strongly adsorbed on cobalt.

The present study used density functional theory (DFT) to study the hydrogenation of nitriles to primary amines on cobalt catalysts and compared the results thus obtained with those reported in a similar study on nickel [6]. The final aim of these calculations was to verify the hypothesis argued in the literature to justify some of the differences observed between nickel- and cobalt-based catalysts.

2. Computational details

We used the Vienna *ab initio* simulation package (VASP) [7,8], which performs an iterative solution of the Kohn–Sham equations in a plane wave basis set. Plane waves with kinetic energy $\leqslant$300 eV were included in the calculation. The exchange-correlation energy was calculated within the generalized gradient approximation (GGA) using the form of the functional proposed by Perdew and Wang [9,10], usually referred to as Perdew–Wang 91 (PW91). The electron–ion interactions for C, N, H, and Co were described by the projector-augmented wave (PAW) method developed by Blöchl [11]. This is essentially an all-electron frozen core method combining the accuracy of all-electron methods and the computational simplicity of the pseudopotential approach, particularly in the implementation of Kresse and Joubert [12]. A first-order Methfessel–Paxton smearing function with a width of about 0.1 eV was used to account for fractional occupancies [13]. Spin-polarized calculations were done to account for the magnetic properties of cobalt. Initially, the relative positions of the metal atoms were fixed as those in the bulk, with an optimized lattice parameter of 3.5207 Å for FCC cobalt. The optimized lattice parameter was calculated using the smallest unit cell possible for modeling the bulk of FCC Co, and its reciprocal space was sampled with a $(15 \times 15 \times 15)$ k-point grid generated automatically using the Monkhorst–Pack method [14].

The Co(111) surface was modeled with a four-layer slab model with four cobalt atoms per layer representing a $p(2 \times 2)$ surface unit cell and a vacuum region of $\sim$10 Å. The reciprocal space of the $p(2 \times 2)$ unit cell was sampled with a $(5 \times 5 \times 1)$ k-points grid generated automatically using the Monkhorst–Pack method. Partial geometry optimizations were performed, including relaxation of the first metal layer, using the RMM–DIIS algorithm [15]. In this method, the forces on the atoms and the stress tensor were used to determine the search directions for finding the equilibrium positions. Geometry optimizations were stopped when the difference in the total energy in two consecutive steps was $<$0.001 eV. The transition states were located in two steps: (1) using the climbing-image nudget elastic band method (CI-NEB) [16] to find likely transition state structures, and (2) refining the structure of the transition state by performing a geometry optimization calculation using a convergence criterion based on the forces acting on the atoms. The transition state structure was deemed converged when the forces acting on the atoms were all $<$0.04 eV/Å for the various degrees of freedom set in the calculation. The molecules in the gas phase (needed to obtain adsorption energies) were calculated using a $10 \times 10 \times 10$ Å^3 cubic unit cell. Spin-polarized calculations were done when needed.

3. Results and discussion

3.1. Hydrogen cyanide (HC≡N)

Several configurations were considered for HCN adsorbed on Co(111). HCN is likely to adsorb either perpendicularly to the surface through the lone-pair of the nitrogen atom or flat with the CN bond parallel or tilted with respect to the metal surface. Different adsorption sites were studied for these orientations: top (t), bridge (b), and hollow hcp (h) and fcc (f).

As was found for HCN adsorbed on Ni(111) [6], the parallel adsorption modes were energetically favored over the perpendicular ones (Table 1). The most stable adsorption state for HCN involved two adjacent hcp and fcc 3-fold hollow sites; hereinafter, this is designated h-η^3(N)-f-η^3(C); $\eta^k(X)$ indicates that atom X interacts with k-surface atoms. As on Ni(111), both h-η^3(N)-f-η^3(C) and f-η^3(N)-h-η^3(C) configurations showed similar adsorption energies. The adsorption energy of the most stable state [h-η^3(N)-f-η^3(C)] on Co(111) was -1.72 eV, which is 0.22 eV more stable than the most stable adsorption mode found on Ni(111). Therefore, HCN is more strongly adsorbed on Co(111) than on Ni(111), which confirms a previous experimental hypothesis about the stronger adsorption of the nitrile group on cobalt catalysts [1,4].

As was found for Ni(111), a quite elongated CN bond was obtained for HCN adsorbed on a h-η^3(N)-f-η^3(C) site. The CN distance was 1.34 Å for HCN adsorbed on this site, whereas on the gas phase geometry [17], it was 1.16 Å (elongation of

Table 1
HCN adsorption on Co(111) in both perpendicular (⊥) and parallel orientations (∥)

Configuration		E_{ads}[a] (eV)	d_{CN}[b] (Å)	d_{CH} (Å)	∠HCN (°)	z–N[c] (Å)	z–C[c] (Å)
⊥	t-η^1(N)	−0.64	1.17 (0.01)	1.07	180	1.91	–
	b-η^2(N)	−0.27	1.19 (0.03)	1.07	180	1.50	–
	h-η^3(N)	−0.25	1.20 (0.04)	1.07	180	1.34	–
	f-η^3(N)	−0.27	1.20 (0.04)	1.07	180	1.37	–
∥	b-η^1(C,N)	−0.86	1.27 (0.11)	1.10	127	1.70	1.79
	h-η^2(C,N)	−1.32	1.32 (0.16)	1.10	124	1.42	1.51
	f-η^2(C,N)	−1.28	1.32 (0.16)	1.10	124	1.46	1.51
	f-η^3(N)-h-η^3(C)	−1.70	1.34 (0.18)	1.11	122	1.28	1.34
	h-η^3(N)-f-η^3(C)	−1.72	1.34 (0.18)	1.11	122	1.25	1.37
Gas phase	Calculated	0.00	1.16 (0.00)	1.08	180	–	–
	Exp. [17]	–	1.156	1.064	180	–	–

[a] Calculated as the energy of the reaction: $HCN_{(g)}$ + adsorption site → $HCN_{(ads)}$.
[b] Δd_{CN} between parentheses is the elongation of the CN bond with respect to the calculated hydrogen cyanide molecule.
[c] z–X is the height of X to the Co(111) surface.

Table 2
H_2CNH adsorption on Co(111)

Configuration		E_{ads}[a] (eV)	d_{CN}[b] (Å)	d_{NH} (Å)	d_{CH} (Å)	∠HCN (°)	∠HCNH (°)	z–N[c] (Å)	z–C[c] (Å)
∥	b-η^1(C,N)	−0.65	1.41(0.13)	1.03	1.11	115	127	1.86	2.00
	f-η^1(N)-f-η^2(C)	−0.76	1.41 (0.13)	1.03	1.13	114	141	1.91	1.71
	f-η^2(N)-f-η^1(C)	−0.95	1.45 (0.17)	1.03	1.11	113	89	1.50	1.88
	h-η^2(N)-h-η^1(C)	−0.96	1.45 (0.17)	1.03	1.11	113	86	1.48	1.86
	h-η^1(N)-h-η^2(C)	−0.78	1.41 (0.13)	1.03	1.13	114	139	1.89	1.69
Gas phase	Calculated	0.00	1.28 (0.00)	1.04	1.11	119	180	–	–
	Exp. [18]	–	1.273	1.023	1.081	119.7	180		

[a] Calculated as the energy of the reaction: $H_2CNH_{(g)}$ + adsorption site → $H_2CNH_{(ads)}$.
[b] Δd_{CN} between parentheses is the elongation of the CN bond with respect to the calculated methanimine molecule.
[c] z–X is the height of X to the Co(111) surface.

0.18 Å). This significant activation also was observed for the f-η^3(N)-h-η^3(C)/h-η^3(N)-f-η^3(C) configurations on Ni(111) [6]. For the most stable configuration, h-η^3(N)-f-η^3(C), the nitrogen atom was at 1.25 Å from the metal surface, and the C atom was 1.37 Å from the metal surface. The HCN angle for this configuration of 122° clearly indicates a change in the hybridization from sp (in the gas phase) to sp^2.

3.2. Methanimine ($H_2C{=}NH$)

For the imine reaction intermediate, the following parallel adsorption modes were considered: b-η^1(C,N), f-η^1(N)-η^2(C), f-η^2(N)-η^1(C), h-η^2(N)-η^1(C), and h-η^1(N)-η^2(C) (Table 2). The most stable adsorption site for methanimine corresponded to an h-η^2(N)-η^1(C) hollow site (E_{ads} of −0.96 eV). In this configuration, both nitrogen and carbon atoms were saturated, with nitrogen interacting with two cobalt surface atoms and carbon interacting with just one cobalt surface atom. As expected, this configuration was (0.18 eV) more stable than the h-η^1(N)-η^2(C) one, in which a N atom interacts with one cobalt atom and a C atom interacts with two cobalt atoms. Another difference between these two configurations was the HCNH dihedral angle, with 86° for the h-η^2(N)-η^1(C) site and 139° for the h-η^1(N)-η^2(C) site. An important activation of the CN bond was found for the h-η^2(N)-η^1(C) configuration, corresponding to an elongation of 0.17 Å with respect to the gas-phase geometry [18].

Interestingly, the energy difference between HCN and the H_2CNH intermediate was 0.76 eV on Co(111), compared with only 0.50 eV on Ni(111) [6]. This difference is caused by the stronger adsorption of HCN on Co(111). This result can be interpreted as reflecting a higher energy requirement on Co(111) for formation of the imine, which could explain the lower activity (lower reaction rate) observed for cobalt catalysts compared with nickel ones [1,4].

3.3. Methylamine (CH_3NH_2)

Methylamine adsorbs on a top site through the nitrogen lone pair. The calculated DFT adsorption energy for this molecule was −0.53 eV on Co(111), very close to the DFT value obtained on Ni(111) (−0.56 eV) [6]. The adsorption energies obtained for HCN and CH_3NH_2 on both metals could explain the differences in selectivity observed between cobalt and nickel catalysts; the stronger adsorption of HCN on cobalt could retard/inhibit the adsorption of methylamine and of the imine intermediates, which is essential to the production of secondary/tertiary amines by condensation reactions [1,4]. Taking into account the DFT adsorption energies, we can rule out the experimental hypothesis in which the difference in adsorption energy for the amine product explains the differing selectivities of nickel and cobalt catalysts [1]. The calculated adsorption geometry of methylamine on Co(111) shows no significant ac-

tivation of this molecule on adsorption, as we already saw for Ni(111). The adsorption geometry is very close to the experimental [17] and calculated gas-phase geometries. Adsorbed methylamine exhibits only a mirror plane (C_s). The NH_2 group is held parallel to the surface plane, and the CH_3 group is tilted away from the surface normal; this geometry was also described for Ni(111) [6].

For comparison, as we had done for Ni(111), we also calculated the adsorption of ammonia on Co(111) and found that is was −0.39 eV, 0.14 eV lower than that of methylamine. We noted the same trend on Ni(111).

3.4. HCN hydrogenation reaction mechanism

The hydrogenation reaction of hydrogen cyanide to methylamine evolves through a methanimine intermediate. This intermediate can be formed by hydrogenation of the carbon atom to yield H_2CN, followed by hydrogenation of the nitrogen atom to form methanimine, or by hydrogenation of the nitrogen atom to give HCNH, followed by hydrogenation on the carbon atom. From methanimine, the hydrogenation reaction can proceed via hydrogenation of the carbon atom to yield H_3CNH, followed by hydrogenation on the nitrogen atom; or by hydrogenation of the nitrogen atom first to form H_2CNH_2, followed by hydrogenation on the carbon atom to give methylamine (Scheme 1).

The first hydrogenation step can yield HCNH (hydrogenation on the nitrogen atom) or H_2CN (hydrogenation on the carbon atom) as products (Fig. 1). These two reaction steps are slightly endothermic; the reaction energy is ∼0.1 eV more endothermic on Co(111) than on Ni(111) [6]. The transition state found for the nitrogen hydrogenation (TS1) has an energy barrier of 1.46 eV, whereas the energy requirement for hydrogenating the carbon atom (TS2) is 1.26 eV (Fig. 1). The geometries and energies of both transition states are similar to those found for the same elementary steps on Ni(111) [6].

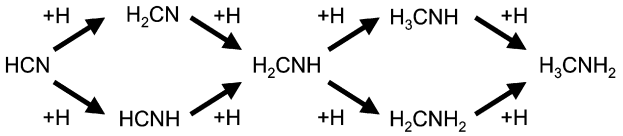

Scheme 1. Reaction intermediates proposed for the hydrogenation reaction of HCN to H_3CNH_2.

Both intermediates formed after HCN hydrogenation, H_2CN and HCNH, are adsorbed on a hollow site; H_2CN on a h-η^3(N) hollow site, and HCNH on a f-η^2(C,N) hollow site (Table 3). Note that there was no preference for the adsorption of H_2CN on either the h-η^3(N) or f-η^3(N) site; the same trend occurred for HCNH at f-η^2(C,N) or at h-η^2(C,N). In the case of H_2CN, the CN bond is perpendicular to the cobalt surface with the nitrogen atom 1.25 Å from the surface, whereas for HCNH, the CN is parallel to the surface and both carbon and nitrogen atoms interact with cobalt atoms (both ∼1.5 Å from the surface). The structures of TS1 and TS2, shown in Fig. 1, demonstrate formation of the N···H and C···H distances (1.45 and 1.38 Å, respectively) and show that the distance between the attacking H atom and the metal surface is 1.60 Å TS1 and 1.50 Å for TS2.

For the second step in the reaction mechanism—the hydrogenation of HCNH or H_2CN to give the imine intermediate—reaction endothermicities of 0.21 and 0.27 eV, respectively, were obtained. For methanimine production, we found it easier to hydrogenate the carbon atom on HCNH than the nitrogen atom on H_2CN; the energy requirements were 0.32 eV for the former (TS3) and 0.84 eV for the latter (TS4) (Fig. 2). The energy barriers found on Ni(111) for the same transition states were slightly higher: 0.44 and 0.96 eV, respectively [6]. The transition state geometries obtained for the two hydrogenation steps were quite close to those found on Ni(111), with a C···H distance of 1.56 Å in TS3 and a N···H distance of 1.46 Å in TS4, with the attacking H atom around 1.4–1.5 Å from the metal surface for both transition states. From the results obtained for the first and second hydrogenation steps, we can conclude that H_2CN is formed preferentially to HCNH ($E_{TS1} > E_{TS2}$), but the hydrogenation of HCNH to H_2CNH is easier than the hydrogenation of H_2CN to H_2CNH ($E_{TS4} > E_{TS3}$). Accordingly, an alternative route in which H_2CN is isomerized to HCNH, which is later hydrogenated to H_2CNH, might be possible.

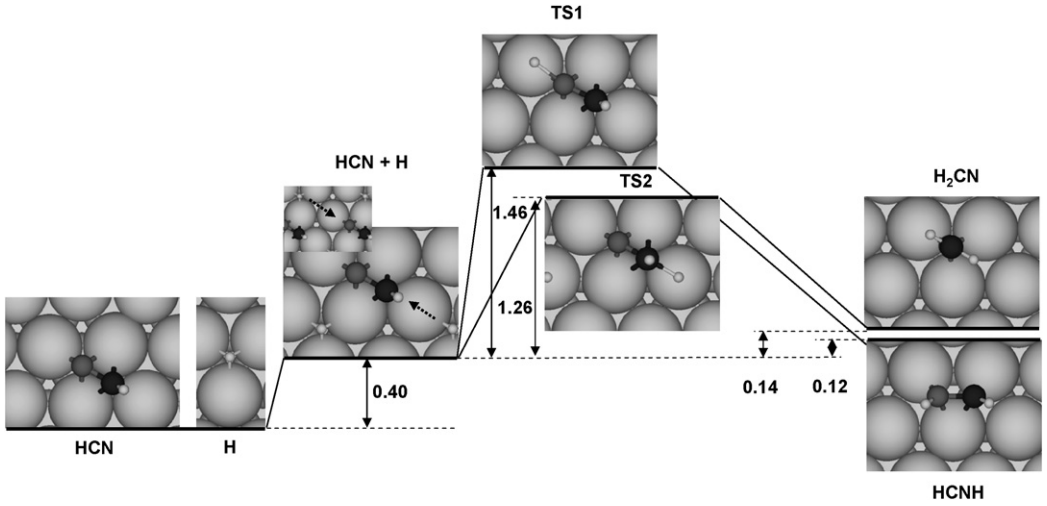

Fig. 1. Energy diagram for $HCN_{(ads)} + H_{(ads)} \rightarrow HCNH_{(ads)}/H_2CN_{(ads)}$.

Table 3
Geometric and energetic data of the intermediates involved in HCN hydrogenation on Co(111)

Configuration		$E_{reaction}$[a] (eV)	d_{CN} (Å)	d_{NH} (Å)	d_{CH} (Å)	∠HCN (°)	∠HNC (°)	∠HCNH (°)	z–N[b] (Å)	z–C[b] (Å)
H_2CN	h-η^3(N)	0.54	1.32	–	1.10	121	–	180	1.18	–
HCNH	f-η^2(C,N)	0.52	1.38	1.03	1.11	118	120	5	1.53	1.45
H_3CNH	b-η^2(N)	0.90	1.48	1.03	1.11	111	107	60	1.59	2.69
H_2CNH_2	f-η^1(N)-f-η^2(C)	1.30	1.49	1.03	1.12	110	112	120	2.04	1.66

[a] Calculated as the energy of the following reactions: $HCN_{(ads)} + 4H_{(ads)} \rightarrow H_2CN_{(ads)} + 3H_{(ads)}$, $HCN_{(ads)} + 4H_{(ads)} \rightarrow HCNH_{(ads)} + 3H_{(ads)}$, $HCN_{(ads)} + 4H_{(ads)} \rightarrow H_3CNH_{(ads)} + 1H_{(ads)}$, $HCN_{(ads)} + 4H_{(ads)} \rightarrow H_2CNH2_{(ads)} + 1H_{(ads)}$.

[b] z–X is the height of X to the Co(111) surface.

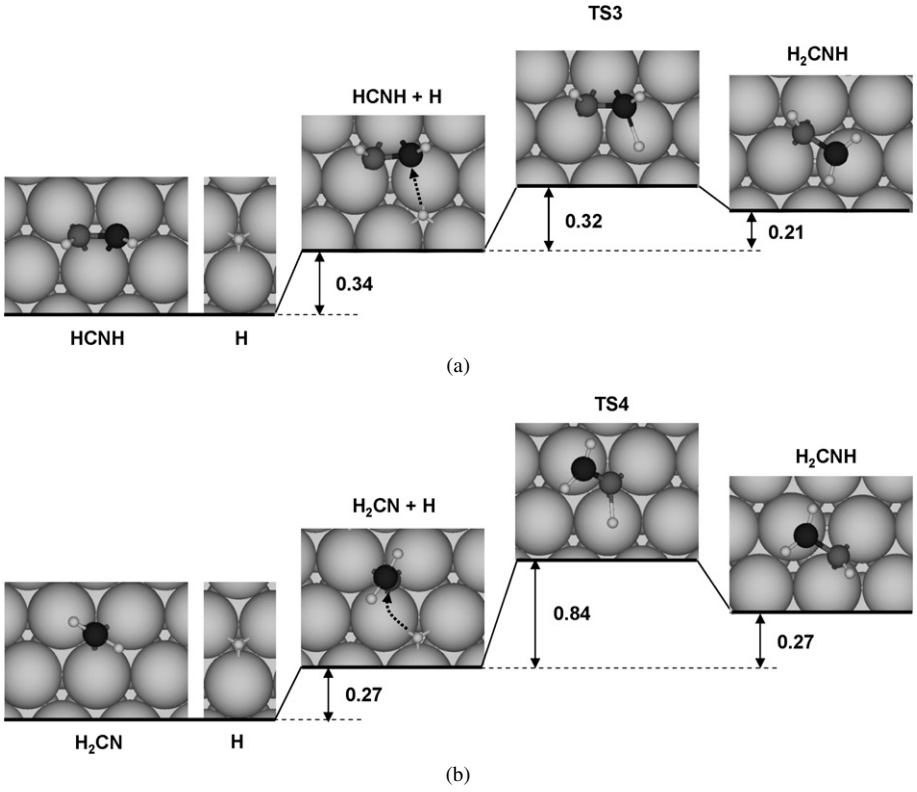

Fig. 2. Energy diagram for (a) $HCNH_{(ads)} + H_{(ads)} \rightarrow H_2CNH_{(ads)}$ and (b) $H_2CN_{(ads)} + H_{(ads)} \rightarrow H_2CNH_{(ads)}$.

The hydrogenation of the imine intermediate formed in the previous step could lead to H_3CNH or H_2CNH_2; the reaction energy was −0.25 eV for H_3CNH production and 0.05 eV for $HCNH_2$ production (Fig. 3). For the H_3CNH intermediate, the preferred adsorption state was b-η^2(N), whereas the H_2CNH_2 intermediate was adsorbed on a hollow f-η^1(N)-f-η^2(C) site (Table 3). In the former intermediate, only the nitrogen atom interacts with the metal surface, whereas for the latter, both carbon and nitrogen atoms interact with the cobalt surface. In both intermediates, the CN distance is already very close to that in methylamine (1.48–1.49 Å). The energies of the transition states found for these reaction steps indicate that hydrogenation on the carbon atom is easier on Co(111) than on Ni(111) [6]. The energy barrier was 1.11 eV for TS5 (H_2CNH_2 production) and 0.51 eV for TS6 (H_3CNH production). As for Ni(111) [6], the structures of the transition states for these reaction steps, TS5 and TS6, can aid understanding of why the nitrogen atom is more difficult to hydrogenate than the carbon atom. Note that both structures are quite similar, with the only difference being in the side of approximation of the attacking H atom. We can conclude that the repulsive interaction between the attacking H atom and the N lone pair is what makes nitrogen hydrogenation more difficult.

The final hydrogenation step corresponds to the attack of hydrogen on the nitrogen atom of H_3CNH or on the carbon atom of H_2CNH_2 to give methylamine (Fig. 4). The formation of CH_3NH_2 from H_3CNH is slightly endothermic, with an energy of reaction of 0.06 eV, whereas the formation of the final amine from H_2CNH_2 is exothermic, with a reaction energy of −0.27 eV. Earlier, we saw that formation of the H_2CNH_2 intermediate was more difficult than formation of the H_3CNH intermediate ($E_{TS5} > E_{TS6}$) but, at the same time, hydrogenation was easier on the carbon atom ($E_{TS7} = 0.76$ eV) than on the nitrogen atom ($E_{TS8} = 1.07$ eV). These results suggest that the H_3CNH intermediate could undergo isomerization on the metal surface to give H_2CNH, which would subsequently give methylamine by hydrogenation. The energies and geometries of the transition states located for these

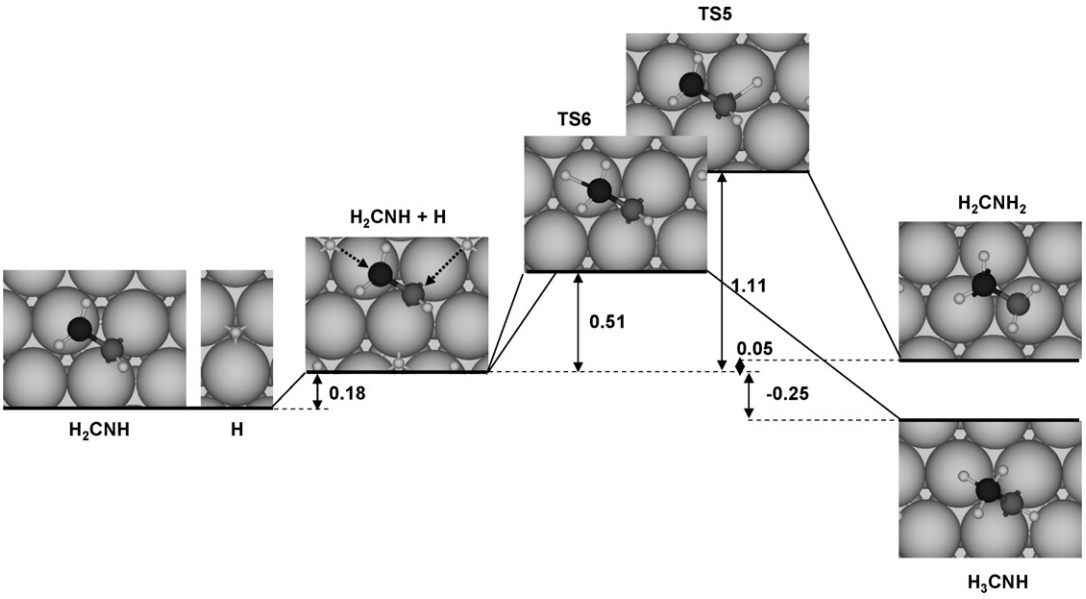

Fig. 3. Energy diagram for $H_2CNH_{(ads)} + H_{(ads)} \rightarrow H_3CNH_{(ads)}/H_2CNH_{2(ads)}$.

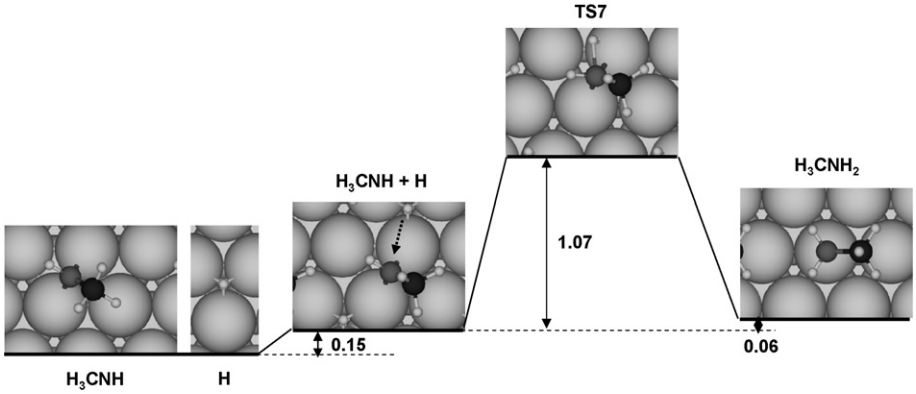

(a)

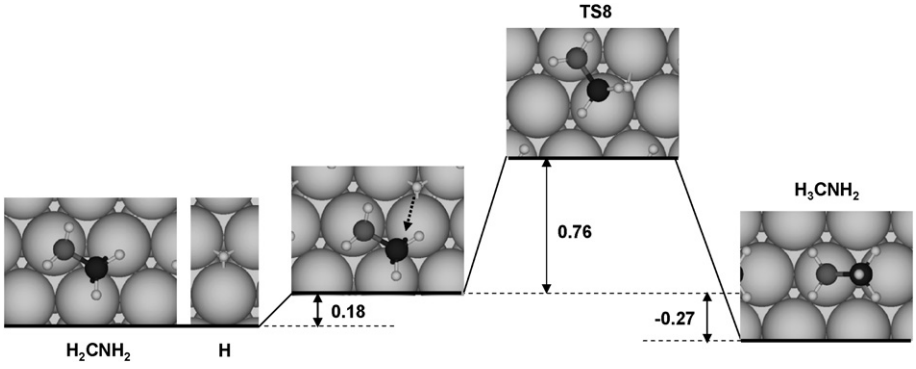

(b)

Fig. 4. Energy diagram for (a) $H_3CNH_{(ads)} + H_{(ads)} \rightarrow H_3CNH_{2(ads)}$ and (b) $H_2CNH_{2(ads)} + H_{(ads)} \rightarrow H_3CNH_{2(ads)}$.

final hydrogenation steps were very similar to those located on Ni(111) [6].

The final step in the reaction mechanism was desorption of the primary amine from the metal surface. The adsorption energy of methylamine on Co(111) was 0.53 eV, very close to the 0.56 eV obtained for Ni(111) [6]. Consequently, the difference in selectivity between the two metals cannot be due to a difference in the adsorption strength of the final primary amine. A full reaction coordinate diagram for the global reaction $HCN + 2H_2 \rightarrow CH_3NH_2$ is shown in Fig. 5, in which the results for Co(111) are compared to those obtained previously for Ni(111) (in *italics*). The reference energy used in the reaction diagram corresponds to the energy of the HCN + 4H system (adsorption energy of HCN plus four

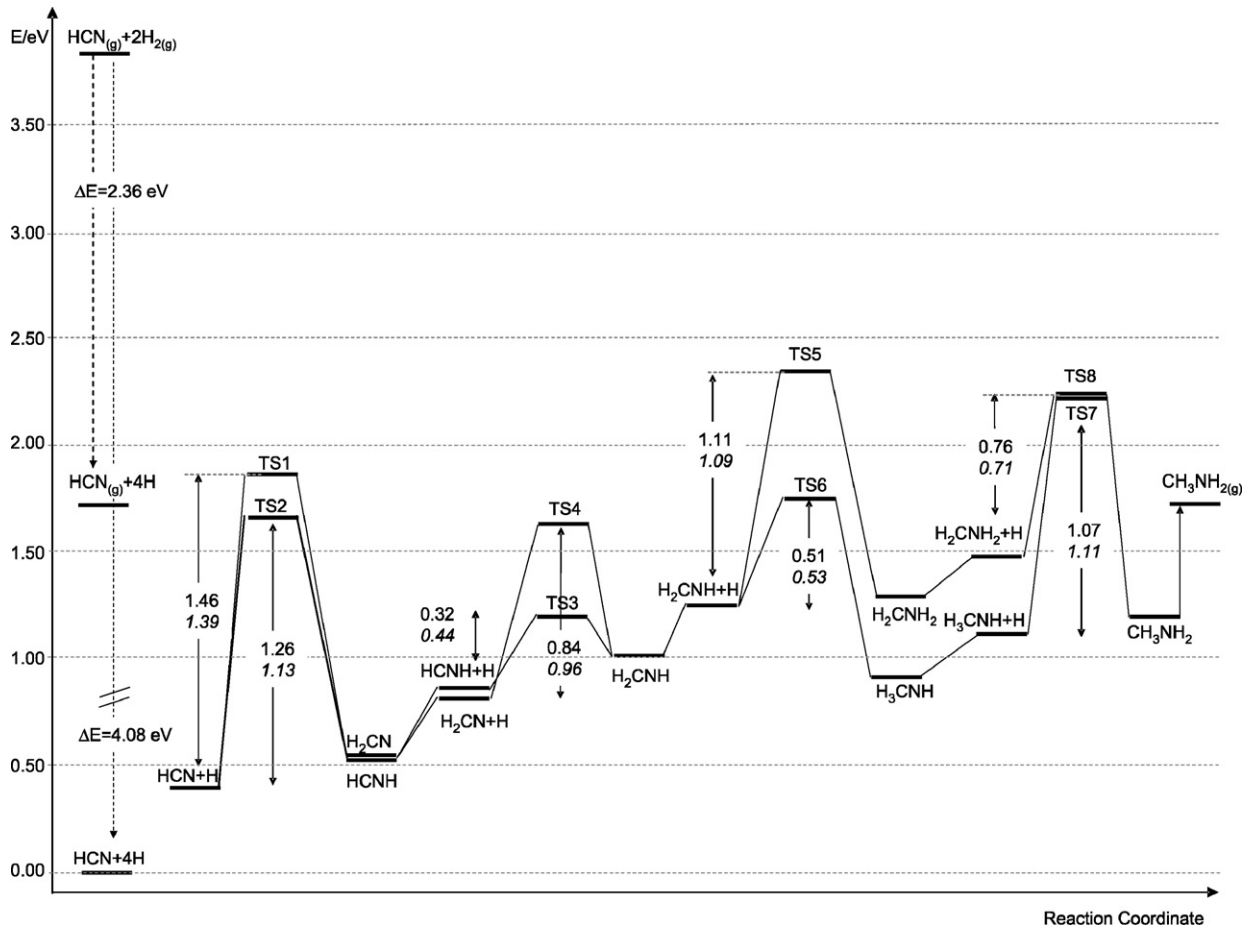

Fig. 5. Reaction energy profile of the hydrogenation of HCN to H_3CNH_2 on Co(111). The values obtained on Ni(111) for the energy barriers are also given in *italics*.

times the adsorption energy of one hydrogen atom). It can be seen that the adsorption energy of HCN was decreased when H was present on the surface; interestingly, the adsorption energy of HCN coadsorbed with hydrogen was slightly larger than the activation energy of formation of H_2CN (TS2) and slightly lower than the activation energy of formation of HCNH (TS1).

3.5. CH_3NH_2 dehydrogenation

The dehydrogenation of methylamine on transition metal surfaces can occur by either N–H or C–H bond cleavage. Experiments have shown that N–H bond-breaking is preferred on metal surfaces such as Pt(111) [19] and Pd(111) [20], whereas C–H bond-breaking has been reported to occur on Ni(111) [21]. In a recent study [6], we showed that the activation energy of C–H bond-breaking is lower than that of N–H bond-breaking on Ni(111), thus confirming the experimental findings. On the other hand, our calculations on Co(111) indicate no such preference on this surface; both the C–H and N–H dehydrogenation steps have similar energy requirements. The calculated activation energy for C–H bond breaking to give $H_2CNH_2 + H$ was 1.02 eV, and the activation energy for N–H bond breaking to give $H_3CNH + H$ was 1.01 eV (reverse reactions for TS7 and TS8 in Fig. 4).

4. Conclusions

This paper has presented a DFT study of the hydrogenation of hydrogen cyanide to methylamine on Co(111). To the best of our knowledge, there are no previous experimental or theoretical studies of this reaction on Co(111). A comparison with our previous theoretical study for the same reaction on Ni(111) was done to help explain the lower activity but higher selectivity observed experimentally for cobalt catalysts compared with nickel catalysts. The main conclusions derived from this work can be summarized as follows:

1. Adsorption of the HCN molecule (reactant) is stronger on Co(111) than on Ni(111). The stronger adsorption of HCN on cobalt may inhibit the adsorption of the final primary amine and/or of the intermediate imines, which are necessary to give secondary amines (byproducts) by condensation. This fact may explain why cobalt-based catalysts are more selective than nickel based catalysts.
2. The adsorption energy of the methanimine intermediate and of the final amine are very similar on the two metals. Consequently, the hydrogenation reaction is more endothermic on Co(111) than on Ni(111). This may explain the lower activity observed on cobalt catalysts compared with nickel catalysts.

3. The different selectivities toward primary amines has been argued in the literature in terms of a stronger adsorption of the amine on nickel than on cobalt. Our calculations show that the adsorption energy of methylamine is very similar on the two metals; thus, we can rule out this hypothesis.
4. The reaction mechanism on the Co(111) surface is very similar to that on the Ni(111) surface. Our calculations show that it is easier to hydrogenate the carbon atom than the nitrogen atom for all of the elementary steps; thus, it may be that two isomerization reactions occur on the catalyst surface: $H_2CN \rightarrow HCNH$ and $H_3CNH \rightarrow H_2CNH_2$.

Acknowledgments

The authors thank the *Stichting Nationale Computerfaciliteiten* (NCF) for providing supercomputing time at SARA, Amsterdam. C.O. acknowledges the European Union for a Marie-Curie Fellowship. D.C. acknowledges support through NWO VENI grant 700-53-403.

References

[1] J. Volf, J. Pasek, in: L. Cerveny (Ed.), Studies in Surface Science and Catalysis, vol. 27, Elsevier, New York, 1986, p. 105 (and references therein).
[2] S. Gomez, J.A. Peters, T. Maschmeyer, Adv. Synth. Catal. 344 (2002) 1037.
[3] J. von Braun, G. Blessing, F. Zobel, Ber. Deutsch. Chem. Ges. 56 (1923) 1988.
[4] H. Li, Y. Wu, Y. Wan, J. Zhang, W. Dai, M. Qiao, Catal. Today 93–95 (2004) 493.
[5] J. Barrault, Y. Pouilloux, Catal. Today (1997) 137.
[6] C. Oliva, C. van den Berg, J.W. Niemanstverdriet, D. Curulla Ferré, J. Catal. 245 (2007) 436.
[7] G. Kresse, J. Hafner, Phys. Rev. B 47 (1993) 558.
[8] G. Kresse, J. Furthmüller, Phys. Rev. B 54 (1996) 11169.
[9] J.P. Perdew, J.A. Chevary, S.H. Vosko, K.A. Jackson, M.R. Pederson, D.J. Singh, C. Fiolhais, Phys. Rev. B 46 (1992) 6671.
[10] Y. Wang, J.P. Perdew, Phys. Rev. B 44 (1991) 13298.
[11] P.E. Blöchl, Phys. Rev. B 50 (1994) 17953.
[12] G. Kresse, J. Joubert, Phys. Rev. B 59 (1999) 1758.
[13] M. Methfessel, A.T. Paxton, Phys. Rev. B 40 (1989) 3616.
[14] H.J. Monkhorst, J.D. Pack, Phys. Rev. B 13 (1972) 5188.
[15] P. Pulay, Chem. Phys. Lett. 73 (1980) 393.
[16] G. Henkelmann, B.P. Uberuaga, H. Jónsson, J. Chem. Phys. 113 (2000) 9901.
[17] G. Herzberg, Electronic Spectra and Electronic Structure of Polyatomic Molecules, Van Nostrand, New York, 1966.
[18] M.D. Harmony, V.W. Laurie, R.L. Kuczkowski, R.H. Schwendeman, D.A. Ramsay, F.J. Lovas, W.J. Lafferty, A.G. Maki, J. Phys. Chem. Ref. Data 8 (1979) 619.
[19] W. Erley, J.C. Hemminger, Surf. Sci. 316 (1994) L1025.
[20] J.J. Chen, N. Winograd, Surf. Sci. 326 (1995) 285.
[21] I. Chorkendorff, J.N. Russell Jr., J.T. Yates Jr., J. Chem. Phys. 86 (1987) 4692.